JAFIB
Original Research
Journal of Atrial Fibrillation

www. jafib.com

Label-free Imaging of Myocardial Remodeling in Atrial Fibrillation Using Nonlinear Optical Microscopy: A Feasibility Study.

Petra Büttner[1], Roberta Galli[2], Daniela Husser[1], Andreas Bollmann[1]

[1]*Department of Electrophysiology, Heart Center Leipzig, Strümpellstraße 39, 04289 Leipzig, Germany.*

[2]*Clinical Sensoring and Monitoring, Department of Anesthesiology and Intensive Care Medicine, Faculty of Medicine Carl Gustav Carus, TU Dresden, Fetscherstraße 74, 01307 Dresden, Germany .*

Abstract

Atrial fibrillation, characterized by rapid disorganized electrical activation of myocardium, is caused by and accompanied by remodeling of myocardial tissue. We applied nonlinear optical microscopy (NLOM) to visualize typical myocardial features and atrial fibrillation effects in order to test anon-destructive imaging technology that in principle can be applied in vivo.Coherent anti-Stokes Raman scattering, endogenous two-photon excited fluorescence, and second harmonic generation were used to inspect unstained human atrial myocardium from three patients who underwent surgical Cox-MAZE procedure with amputation of left atrial appendage. Using NLOM techniques, we collected detail-rich pictures of unstained tissue that enable comprehensive characterization of myocardial characteristics like myocyte structure, collagen and lipofuscin deposition, intercalating disc width, and fatty degradation.

Development of in vivo application of the NLOM technique may represent a revolutionary approach in characterizing atrial fibrillation associated myocardial remodeling with important implications for therapy individualization and monitoring.

Introduction

Atrial fibrillation (AF), the most common clinical arrhythmia, is a progressive disease.The progression of AF is mirrored by: 1) a switch from paroxysmal to persistent AF[1], 2) increased left atrial diameter[2],[3] and 3) myocardial regions with non-uniform conduction detected as low voltage areas[4]-[6]. Those clinical phenotypes associate with worse therapy outcome[7]–[10]. AF progression is underpinned by remodeling of myocardial tissue with fibrosis, fatty degeneration and loss of physiological structure[11],[12]. While the clinical phenotypes mentioned before are mere surrogates of AF progression, the real extent of pathophysiological remodeling remains elusive.At present, standard histology procedures are the only option to directly characterize the remodeling extent. Those procedures involve biopsy-sampling and comprehensive sample processing. Sampling from human ventricles e.g.for characterization of cardiomyopathy is routinely performed and remodeling is then characterized by Masson-Trichrome staining which results in red stained muscle fibers, blue to green collagen, light red pink cytoplasm, and black cell nuclei[13]. Biopsy sampling from the atria for histological examination is not recommended as the atrial wall thickness ranges between 1 and 4 mm[14] making it prone to rupture. Consequently, histological characterization of atrial biopsies from patients was only done in pilot studies[15]. In addition,traditional histological processing is prone to artifacts like shrinkage, geometric distortions, and staining-related artifacts[16],[17]. Large cells and structures like adipocytes, myofibrils or the extra cellular matrix fiber orientation throughout the myocardial wall cannot be assessed together due to slicing in 2-5µm steps. Summarizing a time efficient and non-invasive method for direct visualization of atrial remodeling in vivo would represent a critical break through. With our feasibility study, we want to introduce nonlinear optical microscopy (NLOM) an immediate, non-destructive series of techniques based on multiphoton processes[18]. We applied coherent anti-Stokes Raman scattering (CARS), endogenous two-photon excited fluorescence (TPEF) and second harmonic generation (SHG) to inspect unstained slices of human atrial appendage myocardium ex vivo. CARS detects methylene groups and therefore identifies lipidsand proteins[4], TPEF detects endogenous fluorophores like elastin, SHG detects highly ordered structures lacking of inversion symmetry like fibrillary collagen and myosin[5],[6].

Key Words

Atrial Fibrillation, Coherent Anti-Stokes Raman Scattering, Second Harmonic Generation, Two-Photon Excited Fluorescence.

Corresponding Author

Petra Büttner,Department of Electrophysiology, Heart Center Leipzig, Strümpellstraße 39, 04289 Leipzig, Germany.

Methods

Patient samples

Left atrial appendage samples were from three patients with persistent atrial fibrillation undergoing Cox-MAZE procedure with amputation of left atrial appendage at the Heart Center Leipzig. Patient 1 was a 49year old female with a BMI of 30 kg/m2. Patient 2 was a 68 year old femalewith a BMI of 33 kg/m2. Patient 3 wasa 57 years old male with a BMI of 28 kg/m2. Patients 1 and 2 hadlong standing AF (>24 months) while patient 3 had AF for 6 months before surgery. The study was approved by the local ethics committee and patients signed an informed consent. The samples

were washed in phosphate buffered saline to remove blood, fixed in 4% paraformaldehyde, stored at 4°C in the dark, and processed within two weeks.

Nonlinear optical microscopy

For NLOM, samples were sliced into stripes of about 1mm and placed on glass slides. Drying of the samples during measurements was avoided by a drop of phosphate buffered saline. NLOM was performed using laser excitation provided by two ultrafast Erbium fiber sources with repetition rate of 40 MHz. The pump beam laser (Femto Fiber pro NIR from Toptica Photonics AG, Gräfelfing, Germany) emitted at 781.5 nm with pulse duration of 1.2 ps. The Stokes beam laser used to excite the CARS signal (Femto Fiber pro TNIR from Toptica Photonics AG) was set to 1005 nm and had pulse duration of 0.8 ps. A multiphoton microscope Axio Examiner Z.1 coupled to a scanning module LSM 7 (Carl Zeiss AG, Jena, Germany) was used. A water-immersion 20x apochromatic objective with numerical aperture NA= 1.00 was used. Pump laser power in the sample was 45 mW, Stokes laser power was 0.6 mW. All signals were acquired in reflection configuration using non-descanned detection. The CARS signal was selected using a band pass filter centered on 640 nm with bandwidth of 7 nm. The TPEF signal was acquired in the spectral range 500–550 nm. The SHG signal was selected with a band pass filter centered at 390 nm and bandwidth of 18 nm. 8-bit images were simultaneously acquired for CARS, TPEF and SHG, and then merged in RGB images by coding CARS in red, TPEF in green and SHG in blue. Single field-of view images were acquired with pixel dimension of 0.1 µm, pixel dwell time of 0.4 µs, and 8 averages in order to reduce the noise. For images larger than the field of view, a mosaic was produced with tiling procedure followed by stitching, using functions embedded in the microscope software ZEN (Carl Zeiss AG, Jena, Germany). Z-stacks were acquired in order to comply with lack of sample planarity, and maximum intensity projections of single tile z-stacks were used to build final images.

Results

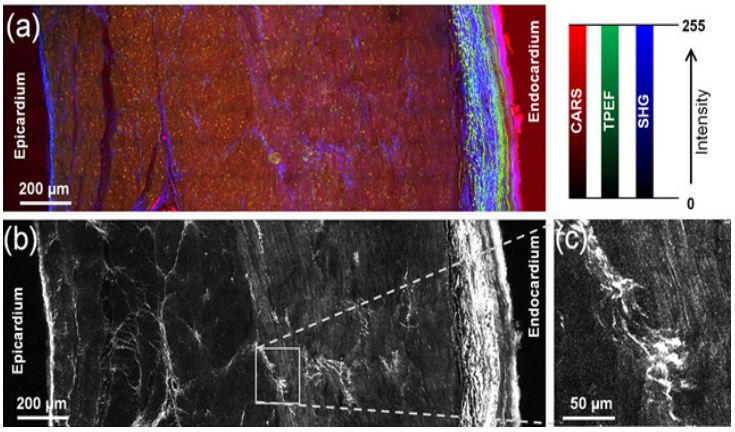

Figure 1: A mosaic of an unstained transmural section of left atrial appendage myocardiumfrom patient 2demonstrating the potential of NLOM. (a) Endocardium, myocardium and epicardium are visualized using CARS (red), endogenous TPEF (green) and SHG (blue). (b) Analysis of collagen and myocytes distribution using SHG (white). (c) Myofibrils orientation and fibrotic remodeling in magnification. The mosaic image was obtained by tiling and stitching of 54 single field-of-view images, each obtained from maximum intensity projection of 22 image planes 10 µm apart. The mosaic image is 3.7 megapixel large. Total acquisition time was about 10 min.

A mosaic of an unstained transmural section of left atrial appendage myocardium was prepared to demonstrate the potential of NLOM techniques[Figure 1]. Endocardium, myocardium and epicardium were visualized at once by simultaneously generated CARS, endogenous TPEF and SHG signals[Figure 1a]. Detection of SHG alone enabled the analysis of disorganized collagen-rich structures and provided a detailed overview of the myocardium morphologywith an apparent myofibril orientation change in the middle of the myocardial wall [Figure 1b] and [Figure 1c].

We further more analyzed atrial cardiomyocytes in detail and observed striation patterns, cell nuclei(which do not produce intense CARS, TPEF or SHG signals whereas they were visible as darker oval bodies), intercalated discs, and a massive accumulation of fluorescent proteins close to the nuclei[Figure 2]. We focused on the intercalated discs[Figure 3] which had an apparent width of 1.0 µm (median of n = 36, 25% percentile = 0.8µm, 75% percentile = 1.1µm, min = 0.7 µm, max = 2.3 µm)on the CARS images, without significant differences among the analyzed patients. Erythrocytes (RBC) localized in small capillaries with diameters of 5-7 µm were also identified by CARS [Figure 3]. Atrial myocardial bundles were also analyzed in cross section [Figure 4]. We observed thin layers of collagen covering the myocyte bundles, peri-nuclear fluorescent protein accumulations, collagen fibers and interstitial lipid droplets with a size of 14 and 17µm. In [Figure 5] typical features of fibrotic remodelingare displayed: increased collagen amount, disorganized elastic fibers, endo-myocardial adipocytes with diameters of 70-100 µm. We finally used SHG microscopy to analyze AF related

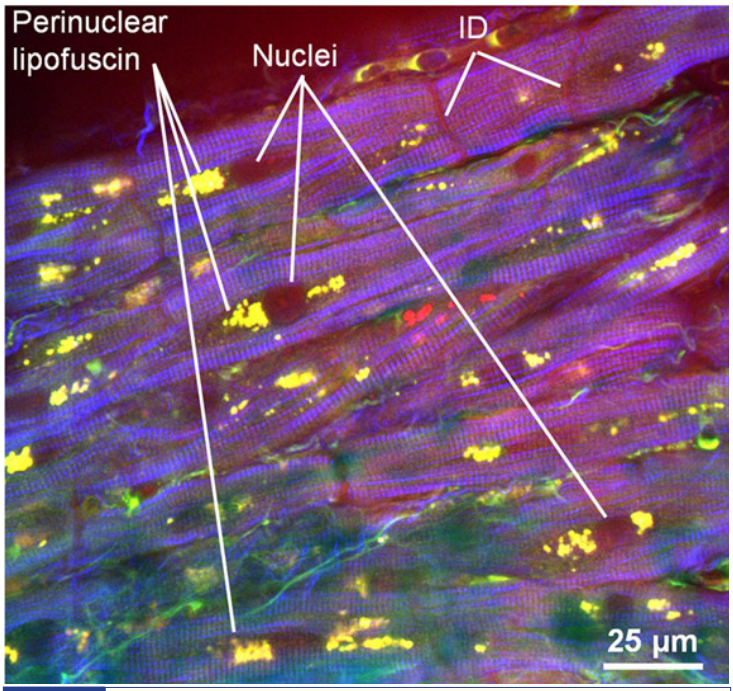

Figure 2: Analysis of unstained atrial cardiomyocytes from patient 1using CARS (red), endogenous TPEF (green) and SHG (blue). Lipofuscin close to the nuclei is detected by both CARS and TPEF, resulting in mixed image colors. ID: intercalating disk.

pathological cardiomyocyte characteristics (figure 6 b) and a virtually intact region [Figure 6a]. Well-defined parallel orientation of cardiomyocytes [Figure 6a] was found as well as degenerative breakup of structure and increased interstitial space where cardiomyocytes

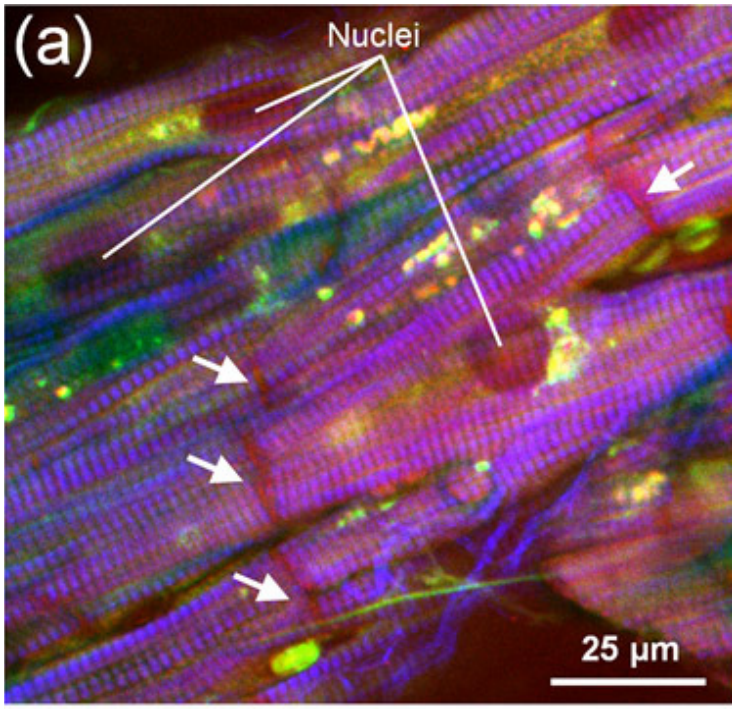

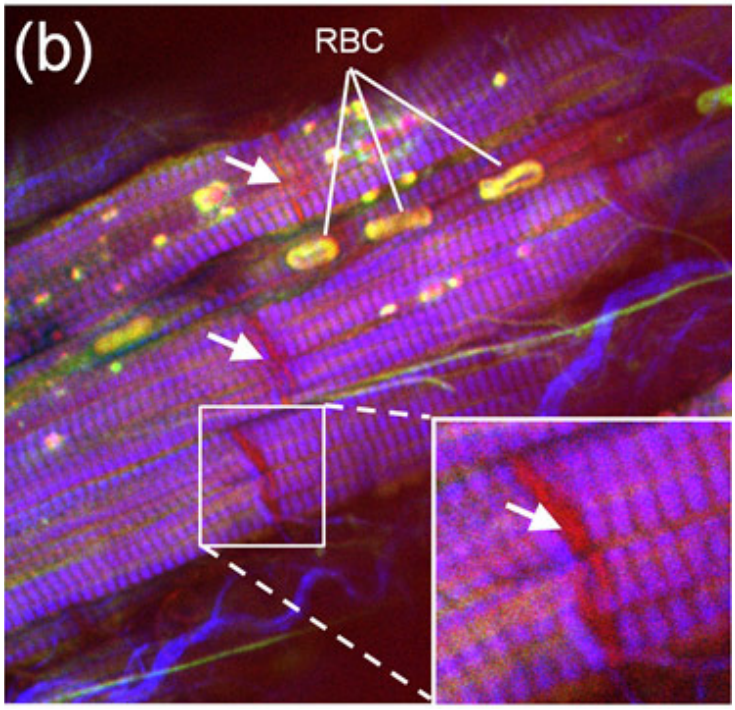

Figure 3: Visualization of intercalating discs in atrial appendage myocardium from patient 3using CARS (red), endogenous TPEF (green) and SHG (blue). (a) Image showing the intercalating discs (arrows). (b) Same sample as in (a), acquired on a different plane (12 µm above), with high magnified details of an intercalating disc. RBC = red blood cells.

lost direct contact, and diffuse collagen fiber bundles marked fibrotic alterations [Figure 6b].

Discussion

Momentarily, cardiomyocytes and myocardium are characterized using fixed thin sample slices which are stained and then visualized using light microscopy or confocal microscopy. Another important technique enabling very detailed analysis is electron-microscopy[19]. All these techniques demand for pre-processing and are prone to

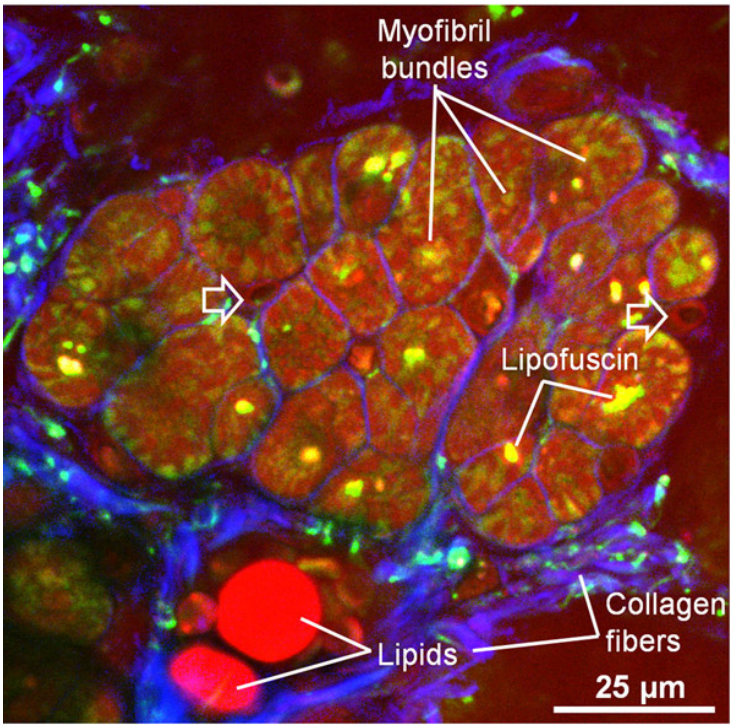

Figure 4: Analysis of unstained atrial cardiomyocytesfrom patient 3 in cross section using CARS (red), endogenous TPEF (green) and SHG (blue). White arrows indicate small capillaries with a diameter of 5-7 µm.

artifacts[16],[17].

With our feasibility study we aimed to demonstrate the potential of NLOM technologies in visualization of established physiological and pathological myocardial features. We visualized myocardium

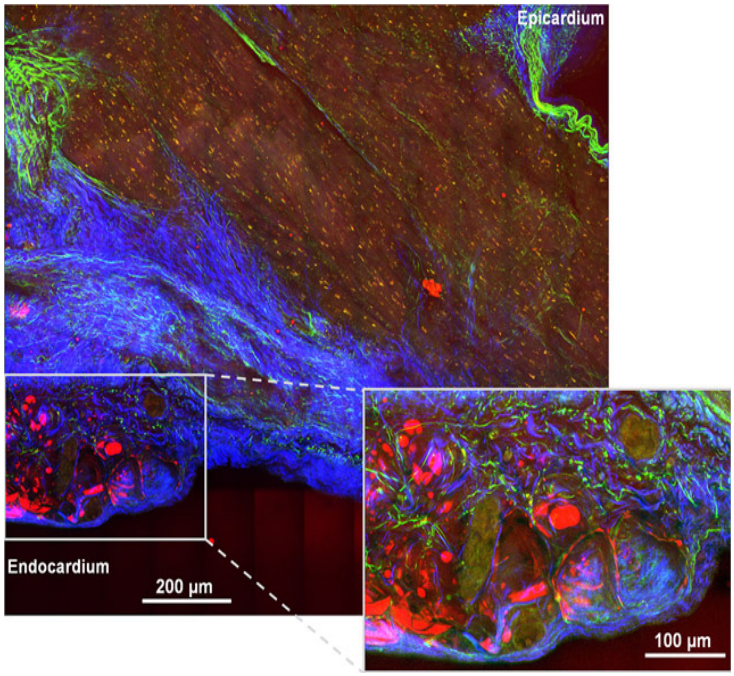

Figure 5: Analysis of a transmural section of atrial myocardium from patient 3showing typical characteristics of fibrotic remodeling using CARS (red), endogenous TPEF (green) and SHG (blue). The mosaic image was obtained by tiling and stitching of 60 single field-of-view images, each obtained from maximum intensity projection of 21 image planes 10 µm apart. The mosaic image is 6.5 megapixels large. Total acquisition time was about 18 min.

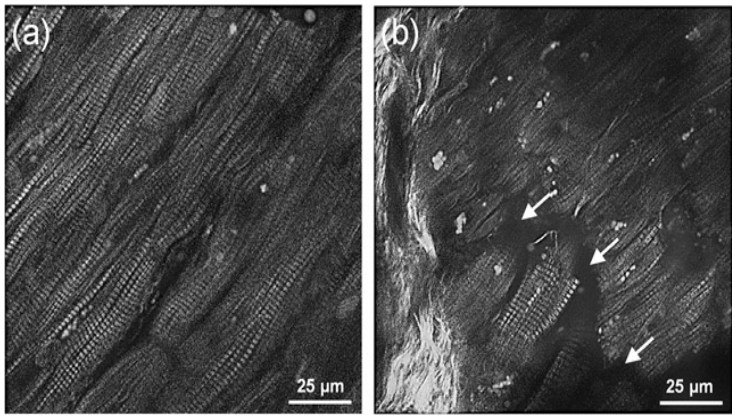

Figure 6: Cardiomyocytes analyzed with SHG (white) (a) Physiological tissue (b) pathological tissue with degenerative alterations (arrows) and fibrotic remodeling (bright white structures on the left side).

at once and cardiomyocytes in detail without pre-processing the tissue except of fixation using paraformaldehyde which we did to prevent tissue decay until measurement took place. Importantly, it had been shown that fixation does not affect NLOM imaging[20]. Simultaneously generated CARS, endogenous TPEF and SHG signals detected collagen and elastin fibers as well as cardiomyocytes, lipid droplets, and adipocytes and collected impressions of myocardial structure, composition and pathological features.

An unexpected finding were massive protein accumulations close to the cardiomyocyte nuclei which were identified to represent lipofuscin characterized by intense endogenous TPEF and by CARS due to the high lipid content[21]. Lipofuscin accumulation as observed in our AF samples is typically regarded as a product of imbalance in disposal and formation in myocardial remodeling processes[22]. Another typical feature of myofibril decay and cardiomyocyte degeneration is intercalated discs alteration[23]. Importantly, in AF the remodeling of intercalated discs is thought to participate in non-uniform electro-conductivity[24]. Standard histological visualization of ID normally demands for staining of ID-specific proteins like plakoglobin[25]. Using NLOMs we observed without any staining clearly visible intercalated discs throughout the myocytes as they produce a strong CARS signal, generated by the dense proteins. Measures of apparent width of 1.0 µm are in line with reported data[24]. Interestingly, we were also able to observe very small intramural capillaries with diameters of 5-7 µm localized between the cardiomyocytes filled with erythrocytes. When we analyzed atrial cardiomyocytes in detailwe observed impressive striation pattern of the myofibrilsusing SHG, with the maximum intensity located at the position of the sarcomere myosin molecules.

Indeed SHG signal is of big interest for the characterization of myocardial pathologies especially fibrotic remodeling. SHG very sufficiently visualizes disorganized collagen-rich structures characteristic for progressing fibrosis in the transmural images and also in the cross sections where anincrease of extra cellular matrix between myocyte bundlesis observed as reported for myocardial disease[26].

Although we analyzed slices of tissue in this study, NLOM in principal is an immediate non-destructive technology with obvious advantages compared to standard histology. As initially stated, biopsy sampling from the atria is complicated because of thin wall structure. In contrast, thin wall thickness is an advantage for NLOM techniques which momentarily enable visualization down to 200 µm depth. Indeed NLOM imaging requires sophisticated set up and is therefore not yet implemented in clinics. Nevertheless, in-vivo application is feasible[27] and development of clinical application in cancerous disease of lung, cervix, skin and gastrointestinal system is recommended[28]. Several groups already work on miniaturization of the technology to transfer it to the clinical application. They report the development of a handheld prototype of a miniature multimodal CARS microscopefor in vivo imaging[29],[30] as well as fiber-based CARS microendoscope[31],[32]. A wearable SHG microscope was also presented[33]. With regards to AF SHG might be the most promising technology for in vivo imaging offibrotic myocardial alterations which are momentarily hardly detectable. Pathological low voltage areas in the atria which are detectable during catheter examinations[9] are regarded to reflect fibrotic remodeling and ablation strategies are already adapted to these findings. We assume that the direct visualization of amounts of collagen indicative for fibrotic remodeling located in low voltage areas would substantially improve the understanding of AF progression. It is not clear whether tissue remodeling and low voltage areas colocalize and by which extent the atrial myocardial wall is affected when low voltage areas are detected. Detailed information could help to further adapt the ablation strategy and to monitor the ablation effect.

Limitations

The study is of preliminary character and was done to test the suitability of NLOM imaging for cardiac disease involving myocardial remodeling. We selected representative images from samples of three patients with persistent AF. We neither compared these patients with each other or healthy individuals nor did we try to detect novel features of pathological alterations. This was beyond the scope of the study.

Conclusion

We show that a combination of the NLOM techniques CARS, SHG and TPEF is very suitable to characterize myocardial remodeling related to AF at macroscopic and cellular level and is at least equal to standard histological characterization without their drawbacks. Consequently, ambitious development of in vivo NLOM technique represents a revolutionary approach with important implications for basic research and individualized therapy.

Acknowledgments

DH and PB were supported by the Volkswagen Foundation, Hanover Germany (grant 84901). We thank Simon Kircher, MD, Martin Misfeld, MD and Thomas Schröter, MD for providing the specimen. We thank Prof. Edmund Koch, PhD and Karin Klingel, MD for their valuable comments.

References

1. Pillarisetti J, Patel A, Boc K, Bommana S, Sawers Y, Vanga S, Sayana H, Chen W, Nath J, Vacek J, Lakkireddy D. Evolution of Paroxysmal Atrial Fibrillation to Persistent or Permanent Atrial Fibrillation: Predictors of Progression. J Atr Fibrillation. 2009;2 (1).
2. Knecht S, Pradella M, Reichlin T, Mühl A, Bossard M, Stieltjes B, Conen D, Bremerich J, Osswald S, Kühne M, Sticherling C. Left atrial anatomy, atrial fibrillation burden, and P-wave duration-relationships and predictors for single-procedure success after pulmonary vein isolation. Europace. 2018;20 (2):271–278.
3. Njoku A, Kannabhiran M, Arora R, Reddy P, Gopinathannair R, Lakkireddy D, Dominic P. Left atrial volume predicts atrial fibrillation recurrence after radiofrequency ablation: a meta-analysis. Europace. 2018;20 (1):33–42.

4. Pezacki JP, Blake JA, Danielson DC, Kennedy DC, Lyn RK, Singaravelu R. Chemical contrast for imaging living systems: molecular vibrations drive CARS microscopy. Nat. Chem. Biol. 2011;7 (3):137–45.
5. Vanzi F, Sacconi L, Cicchi R, Pavone FS. Protein conformation and molecular order probed by second-harmonic-generation microscopy. J Biomed Opt. 2012;17 (6).
6. Vogler N, Heuke S, Bocklitz TW, Schmitt M, Popp J. Multimodal Imaging Spectroscopy of Tissue. Annu Rev Anal Chem (Palo Alto Calif). 2015;8 :359–87.
7. Calkins H, Kuck KH, Cappato R, Brugada J, Camm AJ, Chen SA, Crijns HJ, Damiano RJ, Davies DW, Di Marco J, Edgerton J, Ellenbogen K, Ezekowitz MD, Haines DE, Haissaguerre M, Hindricks G, Iesaka Y, Jackman W, Jalife J, Jais P, Kalman J, Keane D, Kim YH, Kirchhof P, Klein G, Kottkamp H, Kumagai K, Lindsay BD, Mansour M, Marchlinski FE, McCarthy PM, Mont JL, Morady F, Nademanee K, Nakagawa H, Natale A, Nattel S, Packer DL, Pappone C, Prystowsky E, Raviele A, Reddy V, Ruskin JN, Shemin RJ, Tsao HM, Wilber D. 2012 HRS/EHRA/ECAS Expert Consensus Statement on Catheter and Surgical Ablation of Atrial Fibrillation: recommendations for patient selection, procedural techniques, patient management and follow-up, definitions, endpoints, and research trial design. Europace. 2012;14 (4):528–606.
8. Ganesan AN, Shipp NJ, Brooks AG, Kuklik P, Lau DH, Lim HS, Sullivan T, Roberts-Thomson KC, Sanders P. Long-term outcomes of catheter ablation of atrial fibrillation: a systematic review and meta-analysis. J Am Heart Assoc. 2013;2 (2).
9. Rolf S, Kircher S, Arya A, Eitel C, Sommer P, Richter S, Gaspar T, Bollmann A, Altmann D, Piedra C, Hindricks G, Piorkowski C. Tailored atrial substrate modification based on low-voltage areas in catheter ablation of atrial fibrillation. Circ Arrhythm Electrophysiol. 2014;7 (5):825–33.
10. Kirchhof P. Integrated care of patients with atrial fibrillation: the 2016 ESC atrial fibrillation guidelines. Heart. 2017;103 (10):729–731.
11. Weil BR, Ozcan C. Cardiomyocyte Remodeling in Atrial Fibrillation and Hibernating Myocardium: Shared Pathophysiologic Traits Identify Novel Treatment Strategies?. Biomed Res Int. 2015;2015 .
12. Thanigaimani S, Lau DH, Agbaedeng T, Elliott AD, Mahajan R, Sanders P. Molecular mechanisms of atrial fibrosis: implications for the clinic. Expert Rev Cardiovasc Ther. 2017;15 (4):247–256.
13. Schürer S, Klingel K, Sandri M, Majunke N, Besler C, Kandolf R, Lurz P, Luck M, Hertel P, Schuler G, Linke A, Mangner N. Clinical Characteristics, Histopathological Features, and Clinical Outcome of Methamphetamine-Associated Cardiomyopathy. JACC Heart Fail. 2017;5 (6):435–445.
14. Whitaker J, Rajani R, Chubb H, Gabrawi M, Varela M, Wright M, Niederer S, O'Neill MD. The role of myocardial wall thickness in atrial arrhythmogenesis. Europace. 2016;18 (12):1758–1772.
15. Frustaci A, Chimenti C, Bellocci F, Morgante E, Russo MA, Maseri A. Histological substrate of atrial biopsies in patients with lone atrial fibrillation. Circulation. 1997;96 (4):1180–4.
16. West MJ. Tissue shrinkage and stereological studies. Cold Spring Harb Protoc. 2013;2013 (3).
17. Chatterjee S. Artefacts in histopathology. J Oral Maxillofac Pathol. 2014;18 (Suppl 1):S111–6.
18. Zipfel WR, Williams RM, Webb WW. Nonlinear magic: multiphoton microscopy in the biosciences. Nat. Biotechnol. 2003;21 (11):1369–77.
19. Severs NJ. The cardiac muscle cell. Bioessays. 2000;22 (2):188–99.
20. Galli R, Uckermann O, Koch E, Schackert G, Kirsch M, Steiner G. Effects of tissue fixation on coherent anti-Stokes Raman scattering images of brain. J Biomed Opt. 2014;19 (7).
21. Rice WL, Kaplan DL, Georgakoudi I. Two-photon microscopy for non-invasive, quantitative monitoring of stem cell differentiation. PLoS ONE. 2010;5 (4).
22. Terman A, Kurz T, Gustafsson B, Brunk U. The involvement of lysosomes in myocardial aging and disease. Curr Cardiol Rev. 2008;4 (2):107–15.
23. Pluess M, Daeubler G, Dos Remedios CG, Ehler E. Adaptations of cytoarchitecture in human dilated cardiomyopathy. Biophys Rev. 2015;7 (1):25–32.
24. Tribulova N, Egan BT, Szeiffova BB, Viczenczova C, Barancik M. New aspects of pathogenesis of atrial fibrillation: remodelling of intercalated discs. J. Physiol. Pharmacol. 2015;66 (5):625–34.
25. Li J, Radice GL. A new perspective on intercalated disc organization: implications for heart disease. Dermatol Res Pract. 2010;2010 .
26. Alpat S, Yilmaz M, Onder S, Sargon MF, Guvener M, Dogan R, Demircin M, Pasaoglu I. Histologic alterations in tetralogy of Fallot. J Card Surg. 2017;32 (1):38–44.
27. Huff TB, Cheng JX. In vivo coherent anti-Stokes Raman scattering imaging of sciatic nerve tissue. J Microsc. 2007;225 (Pt 2):175–82.
28. Pence I, Mahadevan-Jansen A. Clinical instrumentation and applications of Raman spectroscopy. Chem Soc Rev. 2016;45 (7):1958–79.
29. Murugkar S, Smith B, Srivastava P, Moica A, Naji M, Brideau C, Stys PK, Anis H. Miniaturized multimodal CARS microscope based on MEMS scanning and a single laser source. Opt Express. 2010;18 (23):23796–804.
30. Mittal R, Balu M, Wilder-Smith P, Potma EO. Achromatic miniature lens system for coherent Raman scattering microscopy. Biomed Opt Express. 2013;4 (10):2196–206.
31. Wang Z, Liu Y, Gao L, Chen Y, Luo P, Wong KK, Wong ST. Use of multimode optical fibers for fiber-based coherent anti-Stokes Raman scattering microendoscopy imaging. Opt Lett. 2011;36 (15):2967–9.
32. Lukić A, Dochow S, Chernavskaia O, Latka I, Matthäus C, Schwuchow A, Schmitt M, Popp J. Fiber probe for nonlinear imaging applications. J Biophotonics. 2016;9 (1-2):138–43.
33. Williams JC, Campagnola PJ. Wearable Second Harmonic Generation Imaging: The Sarcomeric Bridge to the Clinic. Neuron. 2015;88 (6):1067–9.